JAERI-Tech
95-004

CALCULATION OF AIR ACTIVATION IN AN ELECTRON LINAC FACILITY USING THE EGS4 CODE SYSTEM

February 1995

Akira ENDO

日本原子力研究所
Japan Atomic Energy Research Institute

本レポートは，日本原子力研究所が不定期に公刊している研究報告書です。

入手の問合わせは，日本原子力研究所技術情報部情報資料課（〒319-11 茨城県那珂郡東海村）あて，お申し越しください。なお，このほかに財団法人原子力弘済会資料センター（〒319-11 茨城県那珂郡東海村日本原子力研究所内）で複写による実費頒布をおこなっております。

This report is issued irregularly.

Inquiries about availability of the reports should be addressed to Information Division, Department of Technical Information, Japan Atomic Energy Research Institute, Tokai-mura, Naka-gun, Ibaraki-ken 319-11, Japan.

編集兼発行　日本原子力研究所

印　　刷　㈱原子力資料サービス

Calculation of Air Activation in an Electron Linac Facility using the EGS4 Code System

Akira ENDO

Department of Health Physics
Tokai Research Establishment
Japan Atomic Energy Research Institute
Tokai-mura, Naka-gun, Ibaraki-ken

(Received January 24, 1995)

Calculations were performed to estimate the concentrations of ^{11}C, ^{13}N and ^{15}O induced through the photonuclear reaction in the air of a target room of an electron linear accelerator facility. The angular distributions of bremsstrahlung spectra from a thick-copper target struck with 100 MeV electrons were estimated using a Monte Carlo code EGS4, and a significant air region where the photonuclear reactions of the air nuclei occur was identified. By use of the photon spectrum in this region, the concentrations of ^{11}C, ^{13}N and ^{15}O were calculated and compared with the experimental results. The calculated values agreed with the measured values within a factor 2.

Keywords: Electron Linear Accelerator, Airborne Radioactivity, EGS4, Photonuclear Reaction, Bremsstrahlung Spectrum

EGS4コードを用いた電子直線加速器施設における空気の放射化量の計算

日本原子力研究所東海研究所保健物理部
遠藤　章

（1995年1月24日受理）

電子直線加速器施設のターゲット室内空気中に，光核反応により生成される ^{11}C，^{13}N 及び ^{15}O の濃度を計算した。100 MeV の電子が銅ターゲットに入射したとき発生する制動放射線スペクトルの角度分布を，電磁カスケードモンテカルロコード EGS4 を用いて計算し，空気の光核反応が起こる領域を特定した。この領域での光子スペクトルを基に ^{11}C，^{13}N 及び ^{15}O の濃度を計算し，実験で測定された濃度と比較した。計算値は，ファクター2以内で実測値と一致した。

東海研究所：〒319－11　茨城県那珂郡東海村白方字白根2－4

Contents

目　　次

1 INTRODUCTION

During the operation of high energy electron accelerators, the primary and secondary particles from the machines produce various radionuclides in air through the photonuclear, spallation and neutron capture reactions [1]. These produced nuclides are present as both aerosols and gases and become a possible source of radiation exposure.

In estimating internal doses due to the intake of these induced airborne radionuclides, their physicochemical properties, such as the particle size of the aerosols and the chemical form of the gases, are significant factors, because the factors affect the transport, deposition and clearance of the inhaled radionuclides in the respiratory tract [2]. Therefore, it is of fundamental interest and importance for the estimation of internal doses in high energy accelerator facilities to clarify the physicochemical properties of the induced airborne radionuclides.

As part of the ongoing interest in the characterization of induced airborne radionuclides, the author measured the compositions of ^{11}C, ^{13}N and ^{15}O and their chemical forms generated by the photonuclear reaction in the air of a 100 MeV electron linear accelerator facility [3]. Based on this experimental study, the author is now developing a kinetic model that describes the chemical compositions of the induced airborne radionuclides. This model requires the photon spectrum and the deposited energy in the air region of concern. These quantities are used to estimate the concentrations of the induced radionuclides and activated species produced by radiolysis of the air molecules that would contribute chemical reactions of the recoiled atoms by the photonuclear reaction.

In this study, simulations by the Monte Carlo method are performed for electromagnetic cascade showers from a thick-copper target struck by a 100 MeV electron beam. The first purpose of the simulations is to clarify the angular distributions of the bremsstrahlung spectra. A significant air region where the photonuclear reaction occurs is identified, and the photon spectrum in the region is calculated. This makes it possible to calculate the concentrations of the induced airborne radionuclides and to compare them with the experimental results. The second purpose is to obtain the deposited energy in the air region that will be used for the kinetic model under development.

2 CALCULATIONS

The number of molecules activated, N^*, by the photonuclear reaction is given by

$$N^* = \phi\sigma N(1 - \exp(-\lambda t_{ir})) , \tag{1}$$

where ϕ is the photon fluence, σ is the cross section of the photonuclear reaction, N is the number of target nuclides in the air region of concern, λ is the decay constant and t_{ir} is the irradiation time of the target nuclide [4, 5]. Procedures for the calculations and estimations of these parameters are given in the following subsections.

2.1 Summary of Experimental Conditions

As described in the introduction, one aim of the present study is to calculate the concentrations of ^{11}C, ^{13}N and ^{15}O to compare them with the experimental values [3].

1 INTRODUCTION

During the operation of high energy electron accelerators, the primary and secondary particles from the machines produce various radionuclides in air through the photonuclear, spallation and neutron capture reactions [1]. These produced nuclides are present as both aerosols and gases and become a possible source of radiation exposure.

In estimating internal doses due to the intake of these induced airborne radionuclides, their physicochemical properties, such as the particle size of the aerosols and the chemical form of the gases, are significant factors, because the factors affect the transport, deposition and clearance of the inhaled radionuclides in the respiratory tract [2]. Therefore, it is of fundamental interest and importance for the estimation of internal doses in high energy accelerator facilities to clarify the physicochemical properties of the induced airborne radionuclides.

As part of the ongoing interest in the characterization of induced airborne radionuclides, the author measured the compositions of ^{11}C, ^{13}N and ^{15}O and their chemical forms generated by the photonuclear reaction in the air of a 100 MeV electron linear accelerator facility [3]. Based on this experimental study, the author is now developing a kinetic model that describes the chemical compositions of the induced airborne radionuclides. This model requires the photon spectrum and the deposited energy in the air region of concern. These quantities are used to estimate the concentrations of the induced radionuclides and activated species produced by radiolysis of the air molecules that would contribute chemical reactions of the recoiled atoms by the photonuclear reaction.

In this study, simulations by the Monte Carlo method are performed for electromagnetic cascade showers from a thick-copper target struck by a 100 MeV electron beam. The first purpose of the simulations is to clarify the angular distributions of the bremsstrahlung spectra. A significant air region where the photonuclear reaction occurs is identified, and the photon spectrum in the region is calculated. This makes it possible to calculate the concentrations of the induced airborne radionuclides and to compare them with the experimental results. The second purpose is to obtain the deposited energy in the air region that will be used for the kinetic model under development.

2 CALCULATIONS

The number of molecules activated, N^*, by the photonuclear reaction is given by

$$N^* = \phi\sigma N(1 - \exp(-\lambda t_{ir})) , \qquad (1)$$

where ϕ is the photon fluence, σ is the cross section of the photonuclear reaction, N is the number of target nuclides in the air region of concern, λ is the decay constant and t_{ir} is the irradiation time of the target nuclide [4, 5]. Procedures for the calculations and estimations of these parameters are given in the following subsections.

2.1 Summary of Experimental Conditions

As described in the introduction, one aim of the present study is to calculate the concentrations of ^{11}C, ^{13}N and ^{15}O to compare them with the experimental values [3].

The calculation requires several parameters which are closely related to the experimental conditions. Therefore, these are briefly outlined below.

Figure 1 shows an overhead view of an electron linac facility of JAERI. Electrons, accelerated by five accelerating tubes, are deflected by a switching magnet and strike on a 6.0 cm thick and 2.2 cm diameter water-cooled copper ($Z = 29$) target where high intensity bremsstrahlung radiation is produced. In the present case, the characteristics of the electron beam were 100 MeV electron kinetic energy, 1 μs pulse width, 50 pps repetition frequency and 10 μA average current.

The target room and the accelerating tube room, which have a capacity of about 400 m^3, were continuously ventilated by fresh air supplied from the exterior of the building at a rate of 1.6×10^4 m^3 h^{-1}. Because of the steady ventilation and the constant electron beam conditions, the radioactive concentration in the air of the target room, which was monitored by a gas flow-through ionization chamber, reached a steady state after 20 min of continuous beam operation.

The activated air was sampled from the target room through a 4 cm diameter and 20 m long sampling pipe, of which the inlet was located about 3 m forward and to the right of the copper target as shown in Figure 1. The air was evacuated with a flow rate of 150 ℓ min^{-1} and introduced to a measuring system placed in a low radiation area outside the concrete shielding. The radioactivity of the aerosol component in the air was measured using a particulate air sampling filter and a plastics scintillation detector, and that of the gaseous component was measured by a gas flow-through ionization chamber.

2.2 Calculations of Bremsstrahlung Spectra and Deposited Energy

The first step for calculating the concentrations of the induced airborne radionuclides is to obtain the photon fluence, ϕ, in the air region of concern. In this subsection, the angular distributions of bremsstrahlung spectra around the copper target are calculated in order to identify the region where the photonuclear reactions of the air nuclei occur, and then the photon spectrum and the deposited energy in the region are calculated.

The most common method for calculating thick-target bremsstrahlung is the use of Monte Carlo techniques. In this study, the EGS4 (Electron Gamma Shower Code Version 4) system [6] was employed. The code system simulates electromagnetic cascade showers in various media by the Monte Carlo method.

Figure 2 shows the geometry for calculating the angular distributions of bremsstrahlung spectra. It consists of a copper target and a 100 cm radius sphere. The electron beam spot is the origin of this coordinate system. The target dimensions are the same as those of the experiment and are 6.0 cm thick and 2.2 cm in diameter. The sphere is divided into 15 regions with respect to the incident beam axis (z axis), that is, 5° intervals from 0° to 30°, 10° intervals from 30° to 90°, and 30° intervals from 90° to 180°. Monoenergetic electrons with a kinetic energy of 100 MeV were supposed to be incident on the central axis of the cylindrical copper target, and photons were emitted from the target by electromagnetic cascade showers. The coordinate at the point of intersection of the sphere and the trajectory of each photon from the target was determined using the `$FINVAL` macro. From the z axis value of the coordinate thus determined, the photon was assigned to the $\theta_j - \theta_{j+1}$ region ($j = 0 - 14 : \theta_0 = 0°, \cdots\cdots, \theta_{15} = 180°$) and was then distributed into 1 MeV-spaced energy bins.

Figure 3 shows the geometry for calculating the photon spectrum and the deposited energy in the air of concern. It consists of the copper target, a 300 cm radius sphere and a cone of which the top is located at the origin of the coordinate system. From the angular distributions of bremsstrahlung spectra from the previously described target, the angle θ was chosen to include the region for the photonuclear reactions of the air nuclei. In the experiment [3], the activated air was evacuated from the sampling port located about 3 m forward and to the right of the copper target (Figure 1) and its radioactivity was measured. The photon spectrum was then calculated at 300 cm forward from the electron beam spot of the copper target using the `$FINVAL` macro. The deposited energy in the air was calculated for the cone region. The cone height was estimated to be 500 cm because the photons emitted from the copper target proceed to the concrete shield that is about 5 m forward of it, as shown in Figure 1.

To perform the above calculations, an EGS4 user code was written on the basis of user codes UCBREM and UCNAI, which were supplied through the courtesy of H.Hirayama of the National Laboratory for High Energy Physics (KEK). The user code includes the following options :

- The PRESTA (**P**arameter **R**educed **E**lectron-**S**tep **T**ransport **A**lgorithm) [7] that treats a path-length correction, a lateral correlation and a boundary-crossing in a charged particle's transport was used to get accurate results. The step size of the charged particles used in all calculations was that chosen by the PRESTA.

- The Ranmar random number generator [8, 9] was used instead of the RAN6, which is used in the standard EGS4, in order to get a long sequence random number. The Ranmar random number generator has a sequence length of about 2×10^{43} and is effective for calculations of a large number of histories.

- The angle of the bremsstrahlung photon relative to the incoming electrons was sampled from the Schiff distribution [10] (the variable `IBRDST=1`), which is essential for obtaining the correct bremsstrahlung angular distribution [11].

- Three sampling methods for the angle of the electron and positron emanating from pair production were applied for comparison. These sampling methods are available in the EGS4 using the variable `IPRDST`, which was introduced by A.F.Bielajew [12]. The first method (`IPRDST=0`) is used in the standard EGS4 and samples with the fixed angle $\Theta_{\pm} = 1/k$, where $\Theta_{\pm}$ is the scattering angle of the e^{+} and e^{-} (in radians) and k is the energy of the initiating photon in units of m_0c^2, the rest mass of the electron. The second one (`IPRDST=1`) samples with the lowest order angular distribution, and the third one (`IPRDST=2`) samples with the Schiff distribution [12, 13]. The latter two methods are able to incorporate the angular distributions of the electron and positron emanating from pair production although they require more computing time than the first method.

- In order to get the data of the position and the energy of each particle, the subroutines `PLOTXYZ` and `GEOMOUT`, and the required statements [14] were incorporated into the user code. The data were used to illustrate radiation tracks produced by electromagnetic cascade showers using a shower display system [14].

The material data used in the EGS4 were calculated with the PEGS4 (**P**reprocessor for **EGS4**). The APRIM option [15] to make radiative stopping powers identical to those of the ICRU Report 37 [16] and the IRAYL option to produce Rayleigh scattering related data were used for all of the materials. Table 1 shows elemental compositions of these materials used in the EGS4 calculations.

The standard deviation of the mean, s, was obtained by

$$s = \sqrt{\frac{\sum_{i=1}^{n}(x_i - \bar{x})^2}{n-1}} \tag{2}$$

where n is the number of data sets, and $\bar{x}$ is their mean value.

Calculations were performed with a UNIX workstation SUN SPARCstation 2. The number of the incident electrons was $1\times10^6 - 1\times10^7$. Electrons and positrons were followed down to 1 MeV kinetic energy and photons down to 100 keV in the bremsstrahlung spectrum calculations, and electrons and positrons were followed down to 50 keV kinetic energy and photons down to 10 keV in the deposited energy calculation. At these energies, the remaining energy of the particles was deposited at that point.

2.3 Cross Sections and Irradiation Time

The most significant reaction of photons with the air nuclei in the energy range under consideration is the photoneutron reaction. The cross section data for the (γ, n) reaction were prepared by the combination of several data [18, 19, 20, 21, 22, 23, 24]. These cross section data were integrated for every 1 MeV width and are listed in Table 2 along with their references. Cross sections over the energy range given in the references were roughly estimated from these data.

The irradiation time of the air nuclei is primarily determined by the relation of the volume of the region of concern and the ventilation rate. Exact estimation of this irradiation time, however, is difficult because the air flow is complicated by the intricate geometry of the room. As a first approximation, let us define the irradiation time, t_{ir}, as that required to exchange 95 % of the air in the region of the photonuclear reaction. The fraction to exchange 95 % of the air in the room is given by

$$1 - 0.95 = 0.05 = \exp\left(-\frac{q_{vent}}{V_r}\, t_{ex}\right) , \tag{3}$$

where q_{vent} is the ventilation rate, V_r is the volume of the room, and t_{ex} is the time required to exchange 95 % of the air. In the linac facility, q_{vent} is 2.7×10^2 m^3 min^{-1} (1.6×10^4 m^3 h^{-1}) and V_r is 400 m^3, therefore, t_{ex} becomes 4.4 min. The volume of the beam cone of concern, V (cm^3), shown in Figure 3, is

$$V = \frac{(500 \times \tan\ \theta)^2 \times \pi \times 500}{3} . \tag{4}$$

The irradiation time, t_{ir} (min), is then given by

$$t_{ir} = \frac{V}{400 \times 10^6} \times 4.4 . \tag{5}$$

2.4 Calculation of Concentrations of Induced Radionuclides

The radioactive concentration of each nuclide was calculated by introducing the calculated photon spectrum, the cross sections and the estimated irradiation time into eqn (1).

The average beam current, I_{av}, was 10 μA, so that the number of electrons incident on the copper target per second, N_{e^-}, is

$$N_{e^-} = \frac{I_{av}}{1.602 \times 10^{-19}} = 6.242 \times 10^{13} . \quad (6)$$

The calculated photon fluence for a single incident electron was then multiplied by the factor N_{e^-}.

In the experiment, the activated air was sampled through the 4 cm diameter and 20 m long sampling pipe from the target room at a rate of 150 ℓ min^{-1}, therefore, the radioactive decay due to the sampling delay should be corrected in order to compare the calculated values with the measured values. Since the volume of the sampling pipe is 2.5×10^4 cm^3 $(2^2 \times \pi \times 20 \times 10^2)$, the air would then reach from the target room to the measuring system with a delay of 0.2 min $(2.5 \times 10^4/150 \times 10^3 = 0.168 \approx 0.2)$. The measured concentrations were consequently multiplied by a factor $1/\exp(-\lambda t_s)$ where t_s is 0.2 min.

3 RESULTS AND DISCUSSION

3.1 Angular Distributions of Bremsstrahlung Spectra

Figures 4(a) – (d) show the tracks of charged particles and photons produced inside the copper target by a single 100 MeV electron. The trajectories of the incident electron, secondary electrons and positrons emanating from pair production, and photons produced by bremsstrahlung process are clearly understandable. Figure 4(e) shows the electromagnetic cascade showers in and around the copper target by 10 incident electrons. It is clear that photons are emitted in all directions but its intensity is high in the forward region of the copper target.

Figure 5 shows the angular dependence of the photon spectra in 15 regions. It can be seen that the hardest photon spectrum appears in the forward direction of the copper target and that the spectrum towards the side and back becomes gradually softer with increasing the angle.

On the basis of Figure 5, the total number of photons produced through electromagnetic cascade showers was plotted as a function of the θ range (Figure 6). Figure 6(a) is the total number of photons produced by a single incident electron. The figure shows that a certain number of the bremsstrahlung photons are emitted from the side and the back of the copper target although their numbers are large in the forward region. From the view point of air activation, a significant energy range in these bremsstrahlung spectra is 10 – 40 MeV, because the cross section of the photoneutron reaction increases for the giant electric dipole resonance. Figure 6(a) was then replotted for the photons that belong to the energy range 10 – 40 MeV (Figure 6(b)). It was found that the number of photons drastically decreases with an increase in the θ and that more than 95 % of the photons are included in the θ range of 0° – 25°. These results suggest

2.4 Calculation of Concentrations of Induced Radionuclides

The radioactive concentration of each nuclide was calculated by introducing the calculated photon spectrum, the cross sections and the estimated irradiation time into eqn (1).

The average beam current, I_{av}, was 10 μA, so that the number of electrons incident on the copper target per second, N_{e^-}, is

$$N_{e^-} = \frac{I_{av}}{1.602 \times 10^{-19}} = 6.242 \times 10^{13} . \qquad (6)$$

The calculated photon fluence for a single incident electron was then multiplied by the factor N_{e^-}.

In the experiment, the activated air was sampled through the 4 cm diameter and 20 m long sampling pipe from the target room at a rate of 150 ℓ min^{-1}, therefore, the radioactive decay due to the sampling delay should be corrected in order to compare the calculated values with the measured values. Since the volume of the sampling pipe is 2.5×10^4 cm^3 $(2^2 \times \pi \times 20 \times 10^2)$, the air would then reach from the target room to the measuring system with a delay of 0.2 min $(2.5 \times 10^4/150 \times 10^3 = 0.168 \approx 0.2)$. The measured concentrations were consequently multiplied by a factor $1/\exp(-\lambda t_s)$ where t_s is 0.2 min.

3 RESULTS AND DISCUSSION

3.1 Angular Distributions of Bremsstrahlung Spectra

Figures 4(a) – (d) show the tracks of charged particles and photons produced inside the copper target by a single 100 MeV electron. The trajectories of the incident electron, secondary electrons and positrons emanating from pair production, and photons produced by bremsstrahlung process are clearly understandable. Figure 4(e) shows the electromagnetic cascade showers in and around the copper target by 10 incident electrons. It is clear that photons are emitted in all directions but its intensity is high in the forward region of the copper target.

Figure 5 shows the angular dependence of the photon spectra in 15 regions. It can be seen that the hardest photon spectrum appears in the forward direction of the copper target and that the spectrum towards the side and back becomes gradually softer with increasing the angle.

On the basis of Figure 5, the total number of photons produced through electromagnetic cascade showers was plotted as a function of the θ range (Figure 6). Figure 6(a) is the total number of photons produced by a single incident electron. The figure shows that a certain number of the bremsstrahlung photons are emitted from the side and the back of the copper target although their numbers are large in the forward region. From the view point of air activation, a significant energy range in these bremsstrahlung spectra is 10 – 40 MeV, because the cross section of the photoneutron reaction increases for the giant electric dipole resonance. Figure 6(a) was then replotted for the photons that belong to the energy range 10 – 40 MeV (Figure 6(b)). It was found that the number of photons drastically decreases with an increase in the θ and that more than 95 % of the photons are included in the θ range of 0° – 25°. These results suggest that most of the bremsstrahlung photons emitted over 25° have energy less than 10 MeV, so that these photons can hardly cause the photoneutron reaction. It is concluded from Figure 6(b) that the significant region for the photoneutron reactions of the air nuclei is the core region within 25° in Figure 3.

3.2 Photon Spectrum and Deposited Energy

Figure 7 shows photon spectra at 300 cm forward of the target with the θ angle of 25° in Figure 3. The difference in these spectra is the sampling methods for pair production as described in the subsection 2.2. It was found that no significant difference in these spectra was observed within the precision of the calculations. The result suggests that the calculated spectra in the present energy range and scoring region are not affected by the sampling methods employed for pair production. The photon spectrum with IPRDST=1 was then used in the following calculation of radioactivity in the air.

The total energy deposited in the air inside the cone region was 0.10 MeV per single incident electron.

3.3 Calculated Concentrations

From the calculations of the angular dependence of bremsstrahlung spectra, the value of θ in Figure 3 was chosen to be 25°. The volume of the beam cone, V, and the irradiation time of the air, t_{ir}, were then estimated to be 2.8×10^7 cm^3 and 0.31 min (19 sec), respectively. The calculated concentrations of ^{11}C, ^{13}N and ^{15}O from eqn (1) are listed in Table 3 along with their experimental values. The calculated concentrations of ^{13}N and ^{15}O agreed well with the measured values within a factor 2. That of ^{11}C, on the other hand, was three orders of magnitude lower compared with the measured value. In case of ^{11}C, it is produced through not only the ^{12}C $(\gamma, n)^{11}$C reaction but also the (γ, spallation) reactions of ^{14}N and ^{16}O [1]. The concentration of ^{11}C produced by the spallation reactions, therefore, was roughly estimated by employing the cross section data [1] and is listed in parentheses. The estimated value becomes the same order as the measured value. Putting these calculated values together, it could be said that the calculations satisfactorily reproduced the experimental values.

The accuracy of the calculated concentrations could be affected by uncertainty in the following factors :

- Irradiation time of the target nuclides in air.

  The concentration is sensitively affected by the factor $(1 - \exp(-\lambda t_{ir}))$ of eqn (1). This is true for nuclides having short half-lives. In the present calculations, the irradiation time, t_{ir}, was estimated by a simple approximation as the relation of the volume of the beam cone for the photonuclear reaction and the ventilation rate. However, the target room has complicated geometry and it would cause stagnation of the air flow in the room. This factor was not considered in the present calculations but is the most important one that contributes to uncertainty of the calculated concentrations.

- Modification of the photon spectrum under the real geometry.

  In the present Monte Carlo simulation, the simplified geometries consisting of the copper target and the air region were considered. In the linac facility, there are accelerator parts and construction materials around the copper target. It would be expected that the photons scattered by these objects cause the difference in the shape of the bremsstrahlung spectrum with the calculated one. These objects in the target room were not taken into consideration because increased computing time would be required. It is presumed, however, that the effect due to this simplification is a minor one compared with the estimation of t_{ir}.

4 CONCLUSIONS

Calculations were performed to estimate the concentrations of ^{11}C, ^{13}N and ^{15}O induced through the photonuclear reaction in the air of a target room of an electron linear accelerator facility. The angular distributions of bremsstrahlung spectra from the cylindrical copper target struck by 100 MeV electrons, calculated with the EGS4 code, showed that the photonuclear reactions of the air nuclei occur in the forward region with a polar angle of $0° - 25°$ at the beam spot of the copper target. The concentrations of ^{13}N and ^{15}O calculated using the photon spectrum in the region agreed with the experimental values within a factor 2. These results show that the bremsstrahlung spectrum given by the Monte Carlo simulation is extremely useful for the evaluation of air activation in accelerator facilities. The deposited energy was also calculated in the air in front of the copper target. The quantity will be used in the kinetic model for chemical reactions of induced airborne radionuclides under development.

Acknowledgements

The author wishes to acknowledge Y.Yamaguchi of the Radiation Dosimetry Division for initiation to the Monte Carlo technique, H.Hirayama of the National Laboratory for High Energy Physics (KEK) for suggestion of coding of EGS4 user code, and A.F.Bielajew of the National Research Council Canada for comments on the use of IPRDST option.

- Modification of the photon spectrum under the real geometry.

  In the present Monte Carlo simulation, the simplified geometries consisting of the copper target and the air region were considered. In the linac facility, there are accelerator parts and construction materials around the copper target. It would be expected that the photons scattered by these objects cause the difference in the shape of the bremsstrahlung spectrum with the calculated one. These objects in the target room were not taken into consideration because increased computing time would be required. It is presumed, however, that the effect due to this simplification is a minor one compared with the estimation of t_{ir}.

4 CONCLUSIONS

Calculations were performed to estimate the concentrations of ^{11}C, ^{13}N and ^{15}O induced through the photonuclear reaction in the air of a target room of an electron linear accelerator facility. The angular distributions of bremsstrahlung spectra from the cylindrical copper target struck by 100 MeV electrons, calculated with the EGS4 code, showed that the photonuclear reactions of the air nuclei occur in the forward region with a polar angle of $0° - 25°$ at the beam spot of the copper target. The concentrations of ^{13}N and ^{15}O calculated using the photon spectrum in the region agreed with the experimental values within a factor 2. These results show that the bremsstrahlung spectrum given by the Monte Carlo simulation is extremely useful for the evaluation of air activation in accelerator facilities. The deposited energy was also calculated in the air in front of the copper target. The quantity will be used in the kinetic model for chemical reactions of induced airborne radionuclides under development.

Acknowledgements

The author wishes to acknowledge Y.Yamaguchi of the Radiation Dosimetry Division for initiation to the Monte Carlo technique, H.Hirayama of the National Laboratory for High Energy Physics (KEK) for suggestion of coding of EGS4 user code, and A.F.Bielajew of the National Research Council Canada for comments on the use of IPRDST option.

References

[1] IAEA. *Radiological safety aspects of the operation of electron linear accelerators.* IAEA Technical Report Series No.188 (1979).

[2] ICRP. *Human respiratory tract model for radiological protection.* ICRP Publication No.66, to be published.

[3] A.Endo, M.Kikuchi, S.Izawa and Y.Ikezawa. *Characteristics of the chemical forms of ^{11}C, ^{13}N and ^{15}O induced in air by the operation of a 100 MeV electron linear accelerator.* Health Phys., **68**, 80–88 (1995).

[4] K.R.Kase. *Radioactive gas production at a 100 MeV electron linac facility.* Health Phys., **13**, 869–876 (1967).

[5] A.Rindi and S.Charalambus. *Airborne radioactivity produced at high-energy accelerators.* Nucl. Instr. Methods, **47**, 227–232 (196).

[6] W.R.Nelson, H.Hirayama and D.W.O.Rogers. *The EGS4 Code System.* SLAC-265 (1985).

[7] A.F.Bielajew and D.W.O.Rogers. *PRESTA: the parameter reduced electron-step transport algorithm for electron Monte Carlo transport.* Nucl. Instr. Methods, **B18**, 165–181 (1987).

[8] G.Marsaglia, A.Zaman and W.W.Tang. *Toward a universal random number generator.* FSU-SCRI-87-50 (1987).

[9] Y.Namito. *On the Ranmar random number (in Japanese).* Abstracts of the fourth EGS4 user's meeting in Japan, 13–16 (1994).

[10] H.W.Koch and J.W.Motz. *Bremsstrahlung cross-section formulas and related data.* Rev. Mod. Phys., **31**, 920–955 (1959).

[11] A.F.Bielajew, R.Mohan and C.S.Chu. *Improved bremsstrahlung photon angular sampling in the EGS4 code system.* NRCC PIRS-0203 (1989).

[12] A.F.Bielajew. *Improved angular sampling for pair production in the EGS4 code system.* NRCC PIRS-0287 (1991).

[13] J.W.Motz, H.A.Olsen and H.W.Koch. *Pair production by photons.* Rev. Mod. Phys., **41**, 581–639 (1969).

[14] H.Hirayama, Y.Namito, S.Ban and R.Ikeda. *EGS shower display system (1) MS-DOS version (in Japanese).* KEK Internal 96-6 (1994).

[15] D.W.O.Rogers, S.Duane, A.F.Bielajew and W.R.Nelson. *Use of ICRU-37/NBS radiative stopping powers in the EGS4 system.* NRCC PIRS-0177 (1989).

[16] ICRU. *Stopping powers for electrons and positrons.* ICRU Report No.37 (1984).

[17] K.Koyama, Y.Okumura, K.Furuta and S.Miyasaka. *Multigroup cross section sets for shield materials (in Japanese).* JAERI-M 6928 (1977).

[18] S.C.Fultz, J.T.Caldwell, B.L.Berman, R.L.Bramblett and R.R.Harvey. *Photoneutron cross sections for* ^{12}C *and* ^{27}Al. Phys. Rev., **143**, 790–796 (1966).

[19] B.C.Cook, J.E.E.Baglin, J.N.Bradford and J.E.Griffin. $^{12}C\ (\gamma,\ n)\ ^{11}C$ *cross section to 65 MeV.* Phys. Rev., **143**, 724–729 (1966).

[20] J.D.King, R.N.H.Haslam and R.W.Parsons. *The gamma-neutron cross section for* ^{14}N. Can. J. Phys., **38**, 231–239 (1960).

[21] E.G.Fuller. *Photonuclear reaction cross sections for* ^{12}C, ^{14}N *and* ^{16}O. Phys. Reports., **127**, 185–231 (1985).

[22] R.L.Bramblett, J.T.Caldwell, R.R.Harvey and S.C.Fultz. *Photoneutron cross sections of* ^{159}Tb *and* ^{16}O. Phys. Rev., **133**, B869–B873 (1964).

[23] J.T.Caldwell, R.L.Bramblett, B.L.Berman, R.R.Harvey and S.C.Fultz. *Cross sections for the ground- and excited-state neutron groups in the reaction* $^{16}O\ (\gamma,\ n)\ ^{15}O$. Phys. Rev. Lett., **15**, 976–979 (1965).

[24] B.C.Cook, J.E.E.Baglin, J.N.Bradford and J.E.Griffin. $^{16}O\ (\gamma,\ n)\ ^{15}O$ *cross section from threshold to 65 MeV.* Phys. Rev., **143**, 712–723 (1966).

Table 1 Material data.

Element	Target	(wt %) Air [17]
H	—	0.001
C	—	0.013
N	—	75.470
O	—	23.233
Ar	—	1.283
Cu	100	—
Density (g cm^{-3})	8.9333	1.2049×10^{-3}
Pressure (Pa)	—	1.0133×10^{5}

Table 3 Concentrations of ^{11}C, ^{13}N and ^{15}O.

Nuclide	Calculated concentration (Bq cm^{-3})	Measured concentration[1] (Bq cm^{-3})
^{11}C	5.8×10^{-5} $(3.2 \times 10^{-2})^{2}$	7.9×10^{-2}
^{13}N	4.0×10^{-1}	2.7×10^{-1}
^{15}O	7.9×10^{-1}	1.3

1 Decay corrected values of the experimental data. The concentration of each nuclide is the sum of the aerosol and gaseous components [3].

2 The concentration in parentheses is the ^{11}C produced through the (γ, spallation) reactions of ^{14}N and ^{16}O.

Table 2 Cross sections for photoneutron reaction.

Energy bin (MeV)	$^{12}C(\gamma, n)^{11}C$	$^{14}N(\gamma, n)^{13}N$ (mb MeV^{-1})	$^{16}O(\gamma, n)^{15}O$
10 - 11	—	0.008	—
11 - 12	—	0.163	—
12 - 13	—	0.434	—
13 - 14	—	0.528	—
14 - 15	—	0.318	—
15 - 16	—	0.397	0.035
16 - 17	—	0.215	0.310
17 - 18	—	0.569	1.057
18 - 19	0.037	1.443	0.630
19 - 20	0.499	1.903	1.223
20 - 21	1.386	1.687	1.343
21 - 22	4.661	2.031	2.750
22 - 23	6.966	2.859	6.946
23 - 24	6.520	2.770	6.488
24 - 25	4.078	1.748	6.958
25 - 26	3.940	0.772	6.014
26 - 27	3.288	0.511	4.695
27 - 28	2.559	0.446	3.806
28 - 29	2.327	0.381	3.020
29 - 30	2.306	0.337	2.789
30 - 35	1.8	0.2	1.9
35 - 40	1.1	0.2	1.1
40 - 50	1.0	0.2	0.6
50 - 100	0.5	0.2	0.5

$^{12}C(\gamma, n)^{11}C$: threshold - 30 MeV [18], 30 - 65 MeV [19].
$^{14}N(\gamma, n)^{13}N$: threshold - 25 MeV [20], 25 - 30 MeV [21].
$^{16}O(\gamma, n)^{15}O$: threshold - 30 MeV [22, 23], 30 - 65 MeV [24].

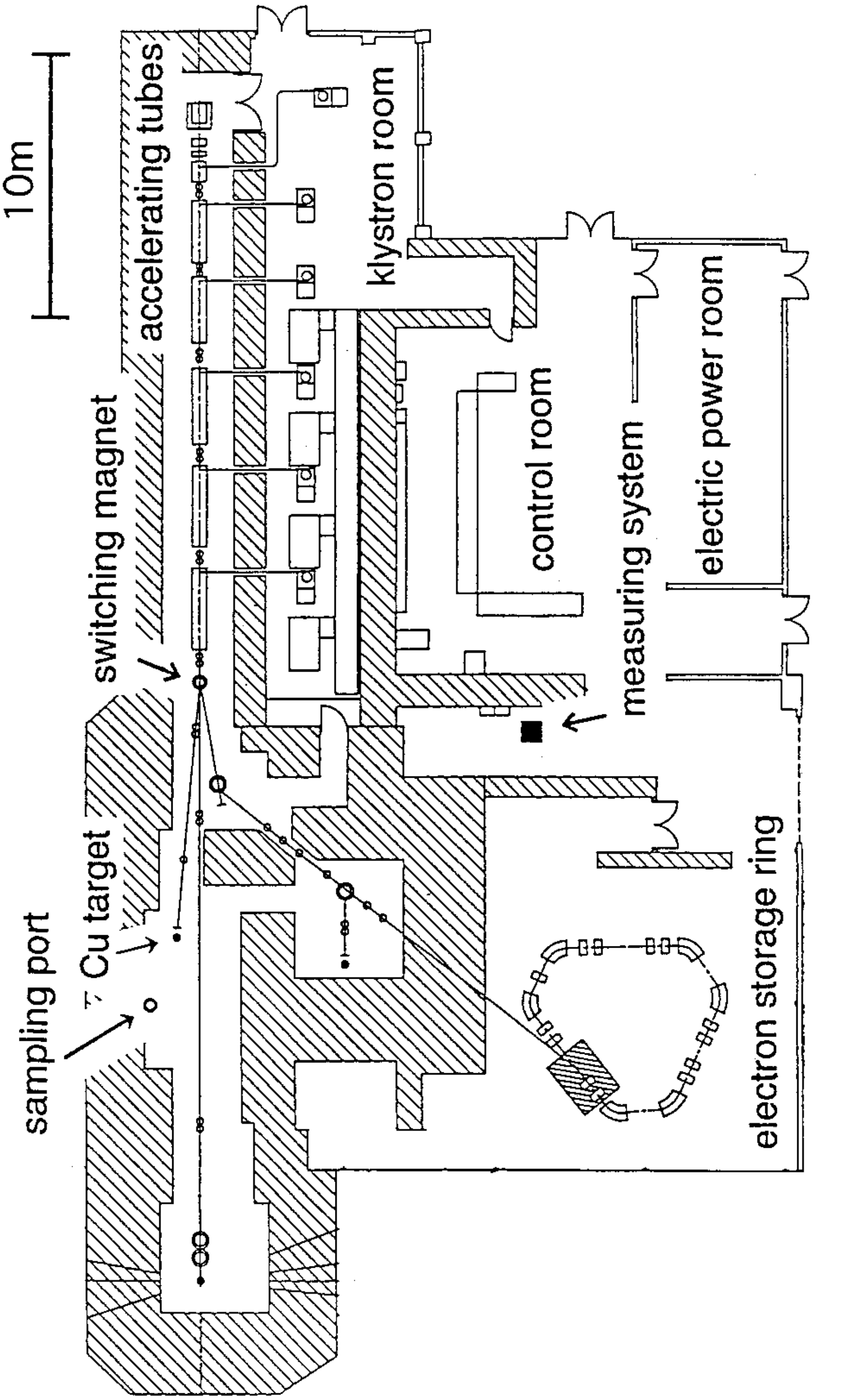

Figure 1 JAERI electron linac facility.

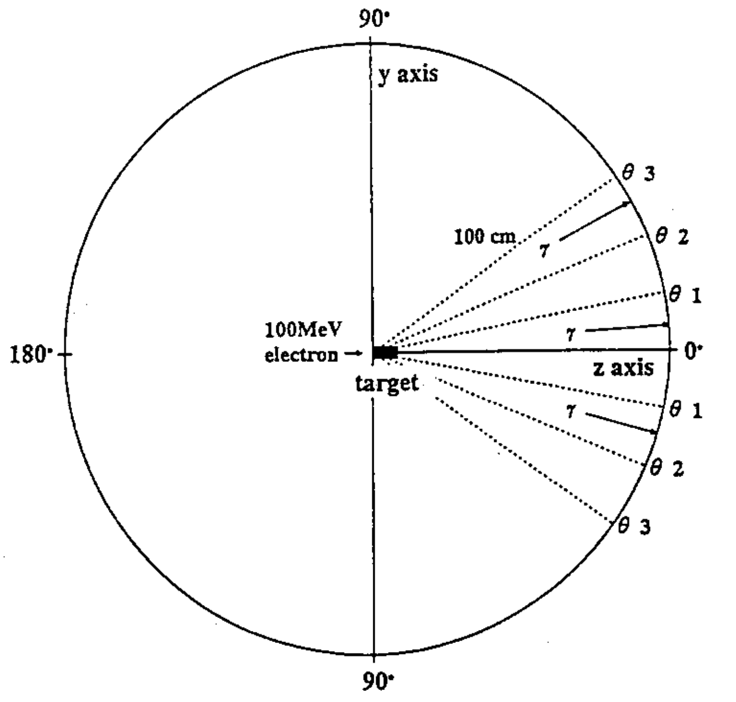

Figure 2　Calculation geometry for the angular dependence of bremsstrahlung spectra.

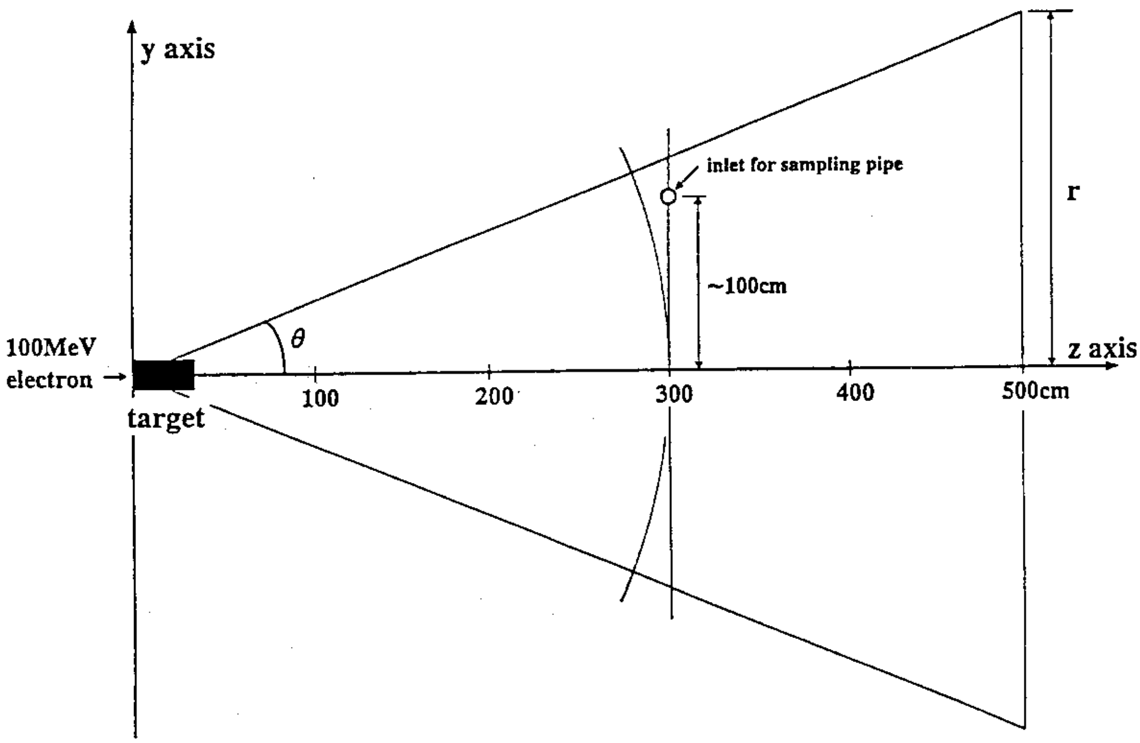

Figure 3　Calculation geometry for the photon spectrum and the deposited energy in the region of concern.

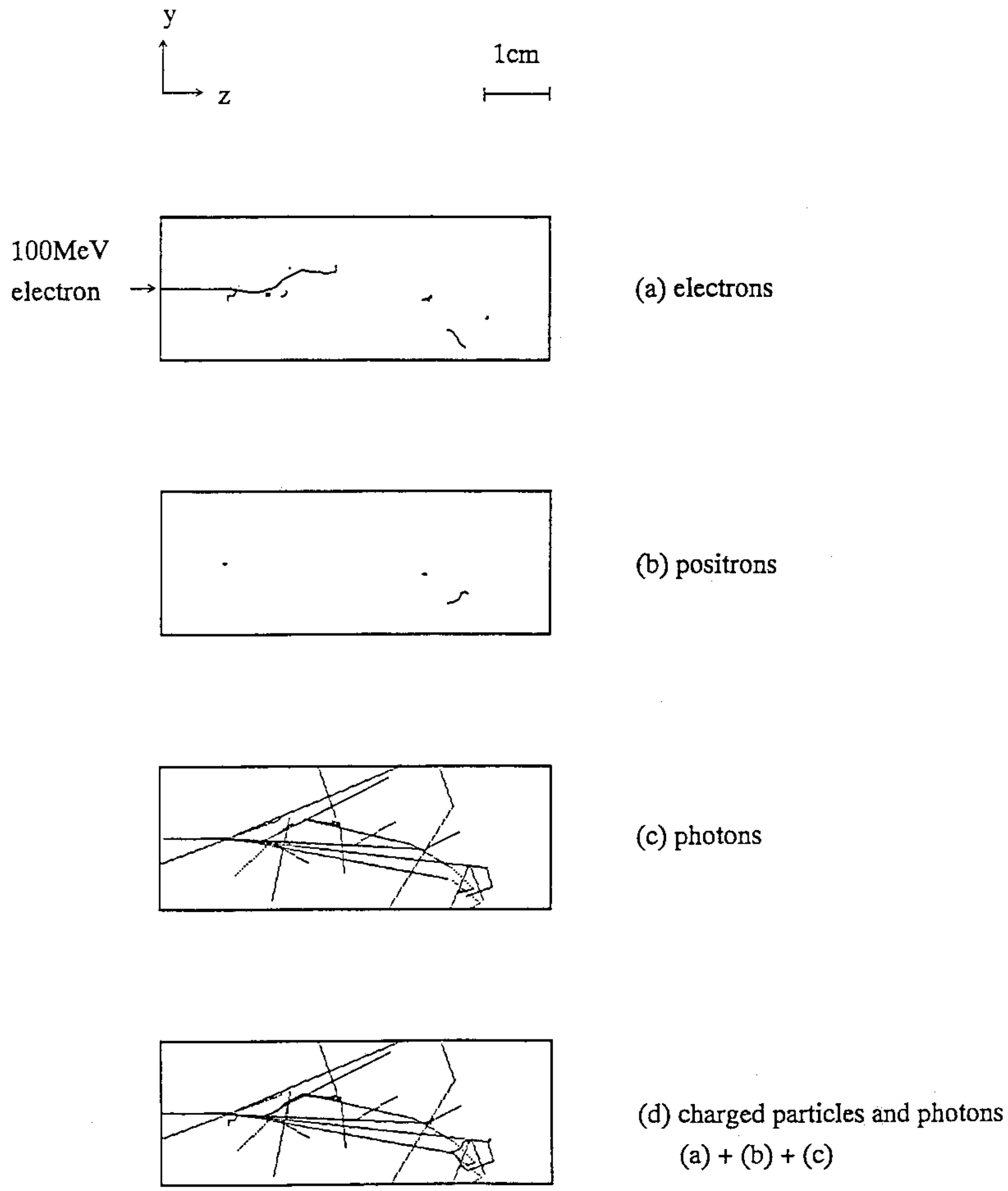

Figure 4 Radiation tracks of charged particles and photons produced through electromagnetic cascade showers by a single 100 MeV electron.

(a)–(d) Tracks inside the copper target.

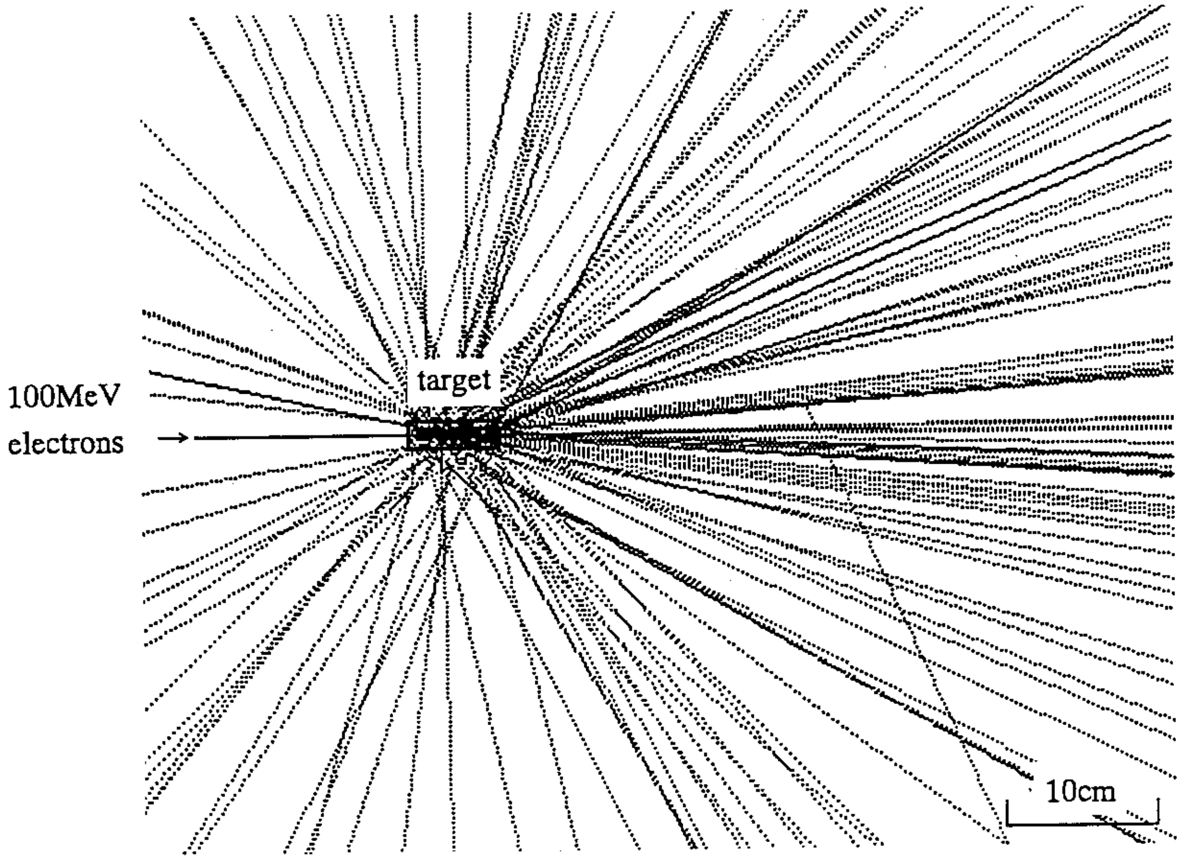

Figure 4 – continued

(e) Tracks inside and around the copper target. Solid lines, charged particles; dotted lines, photons.

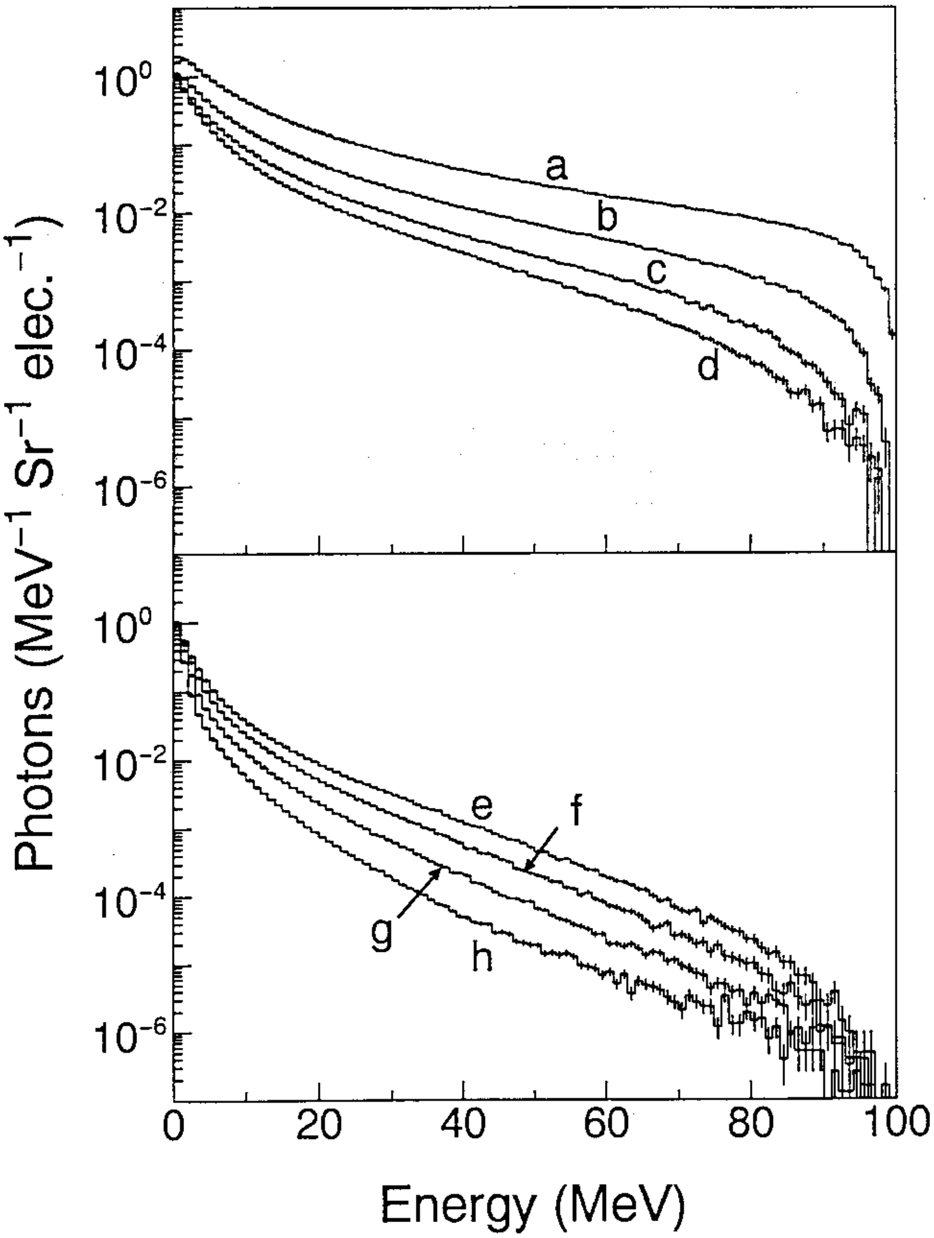

Figure 5 Angular dependence of bremsstrahlung spectra.

1×10^7 electrons were incident on the copper target. Calculations were performed with IPRDST=1. (a) 0° − 5°, (b) 5° − 10°, (c) 10° − 15°, (d) 15° − 20°, (e) 20° − 25°, (f) 25° − 30°, (g) 30° − 40°, (h) 40° − 50°.

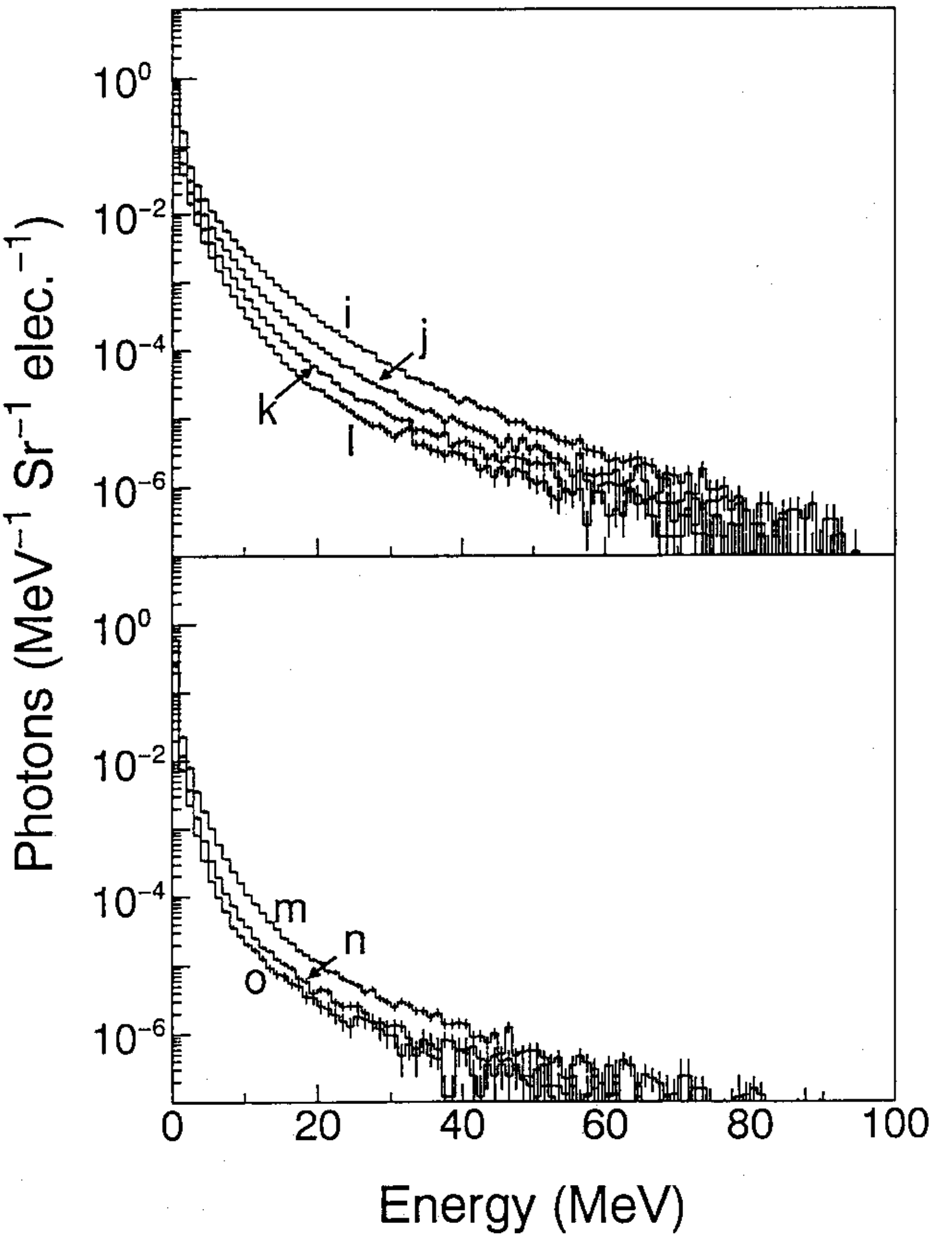

Figure 5 – continued
(i) 50° – 60°, (j) 60° – 70°, (k) 70° – 80°, (l) 80° – 90°, (m) 90° – 120°, (n) 120° – 150°, (o) 150° – 180°.

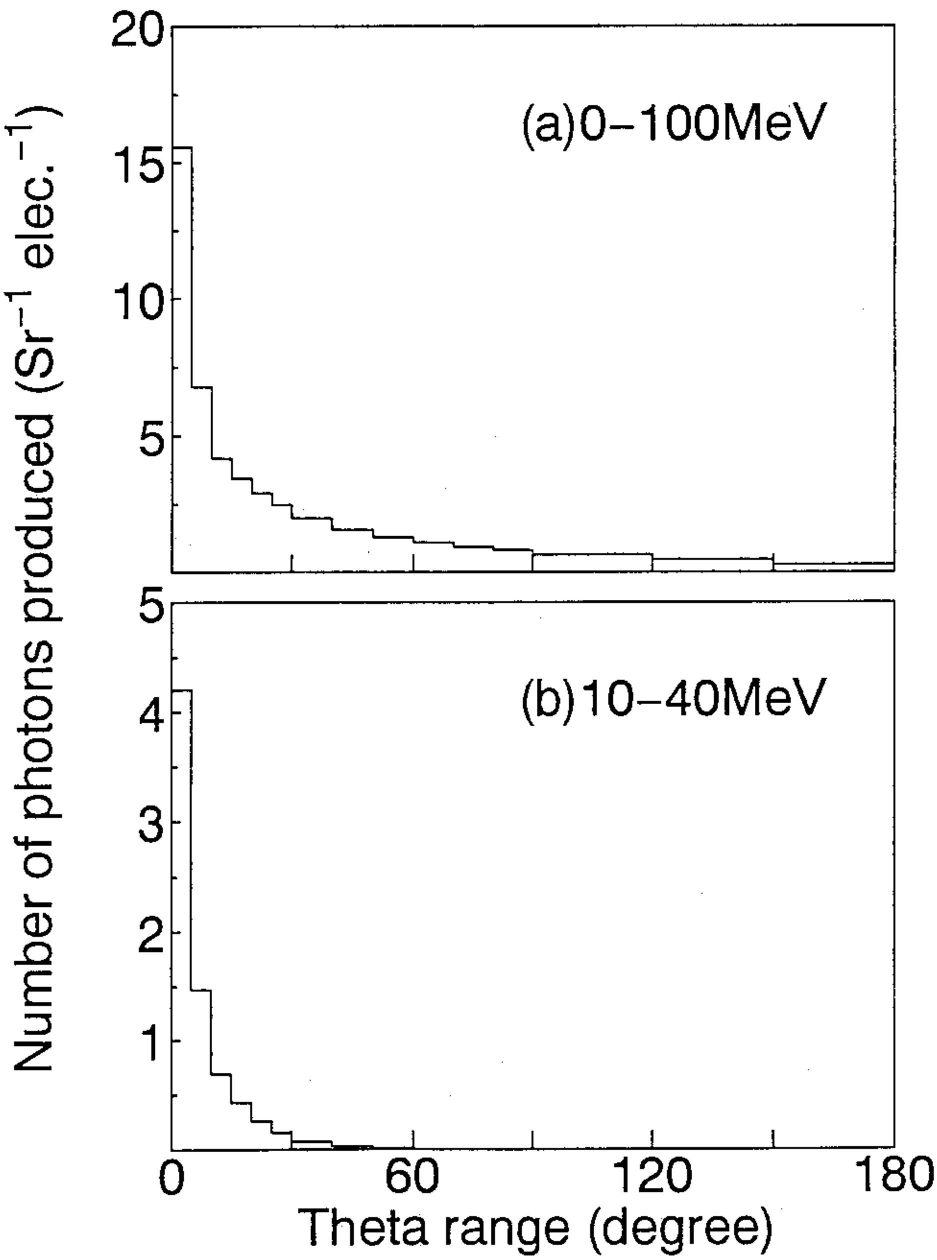

Figure 6 Total number of photons produced through electromagnetic cascade showers by a single 100 MeV electron as a function of θ range.
(a) 0 – 100 MeV, (b) 10 – 40 MeV.

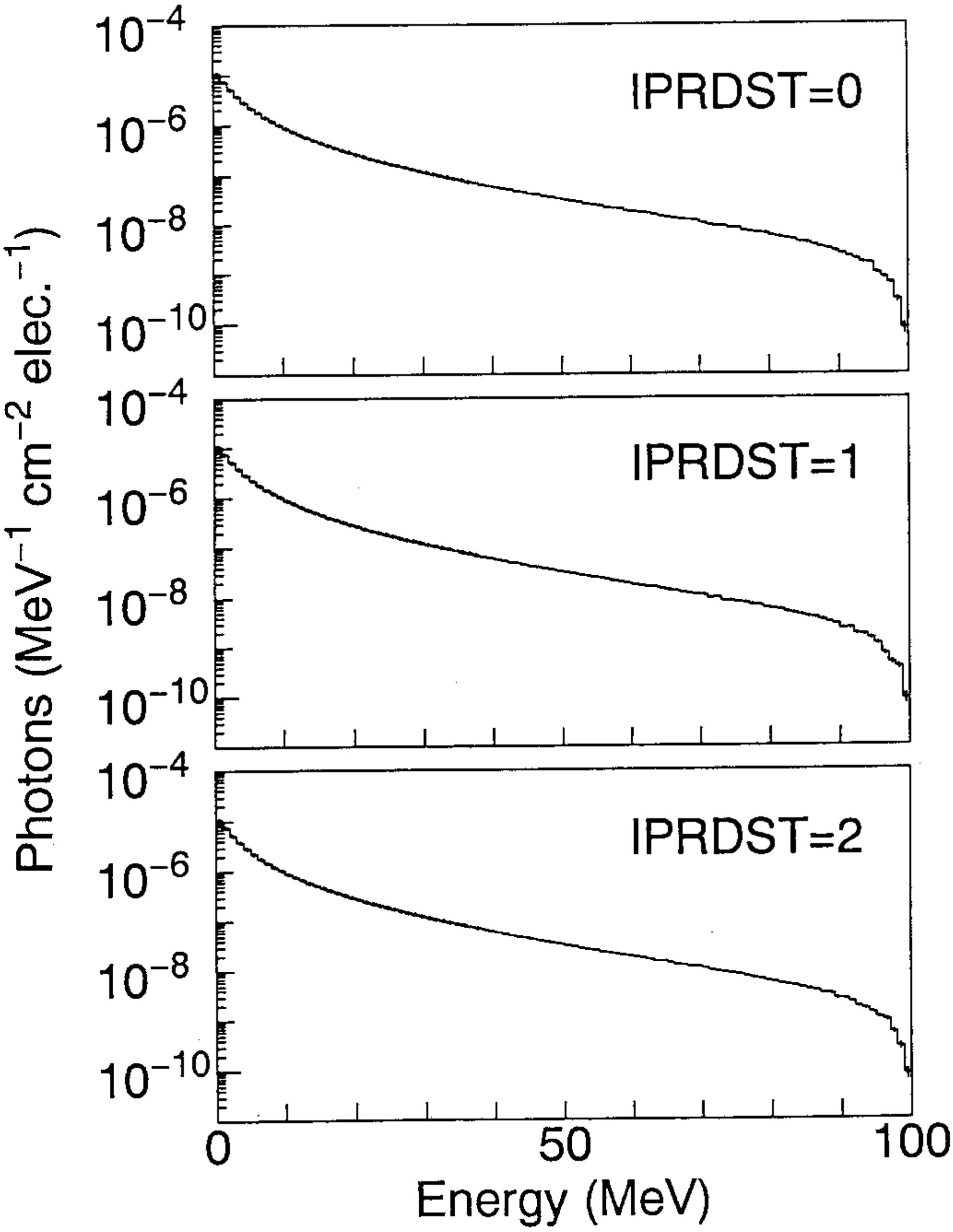

Figure 7 Photon spectra at 300 cm from the beam spot of the copper target with 25° of θ.

5×10^6 electrons were incident on the copper target. Three angular sampling methods for pair production were applied for comparison.